

Supporting Information for

Impact of Varying the Core–Shell Structural Sequence on the Efficiency of Cascade Reagent-Free Fenton-like Oxidation: The Case of Magnetically Recycling Resorcinol–Formaldehyde Resins/Magnetite Composite Microspheres

Liang Yang, Yanlong Wang, Tingyu Chen, Lifang Liu, Yun Cai, Jun Fang* and Yang Yang*

State Key Laboratory of Materials-Oriented Chemical Engineering, College of Chemical Engineering, Nanjing Tech University, No. 30 Puzhu South Road, Nanjing 211816, P. R. China

*Corresponding author: Prof. Dr. Jun Fang E-mail: fangjun@njtech.edu.cn

Prof. Dr. Yang Yang E-mail: yangy@njtech.edu.cn

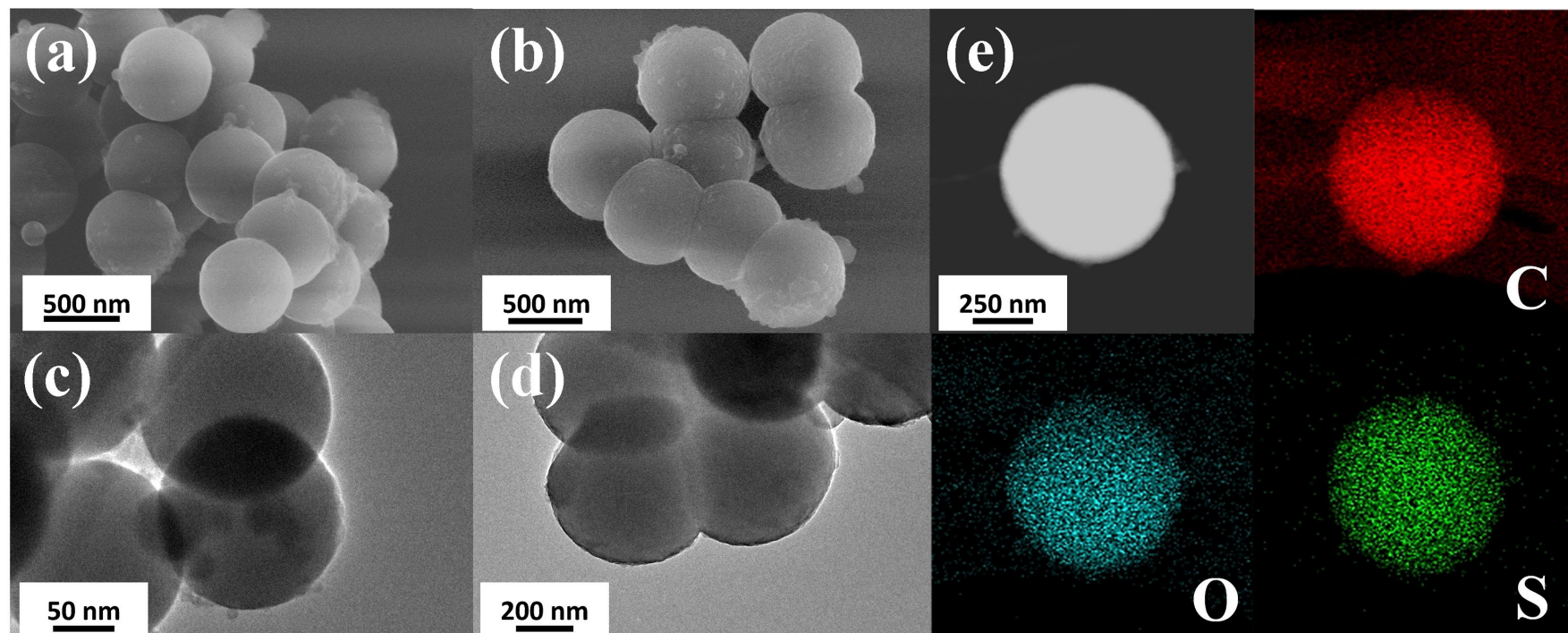


Fig. S1 SEM images of (a) RF and (b) sulfonated RF resin microspheres. TEM images of (c) RF and (d) sulfonated RF resin microspheres. (e) HADDF-STEM image and the EDX elemental mappings of RF resin microspheres after sulfonation.

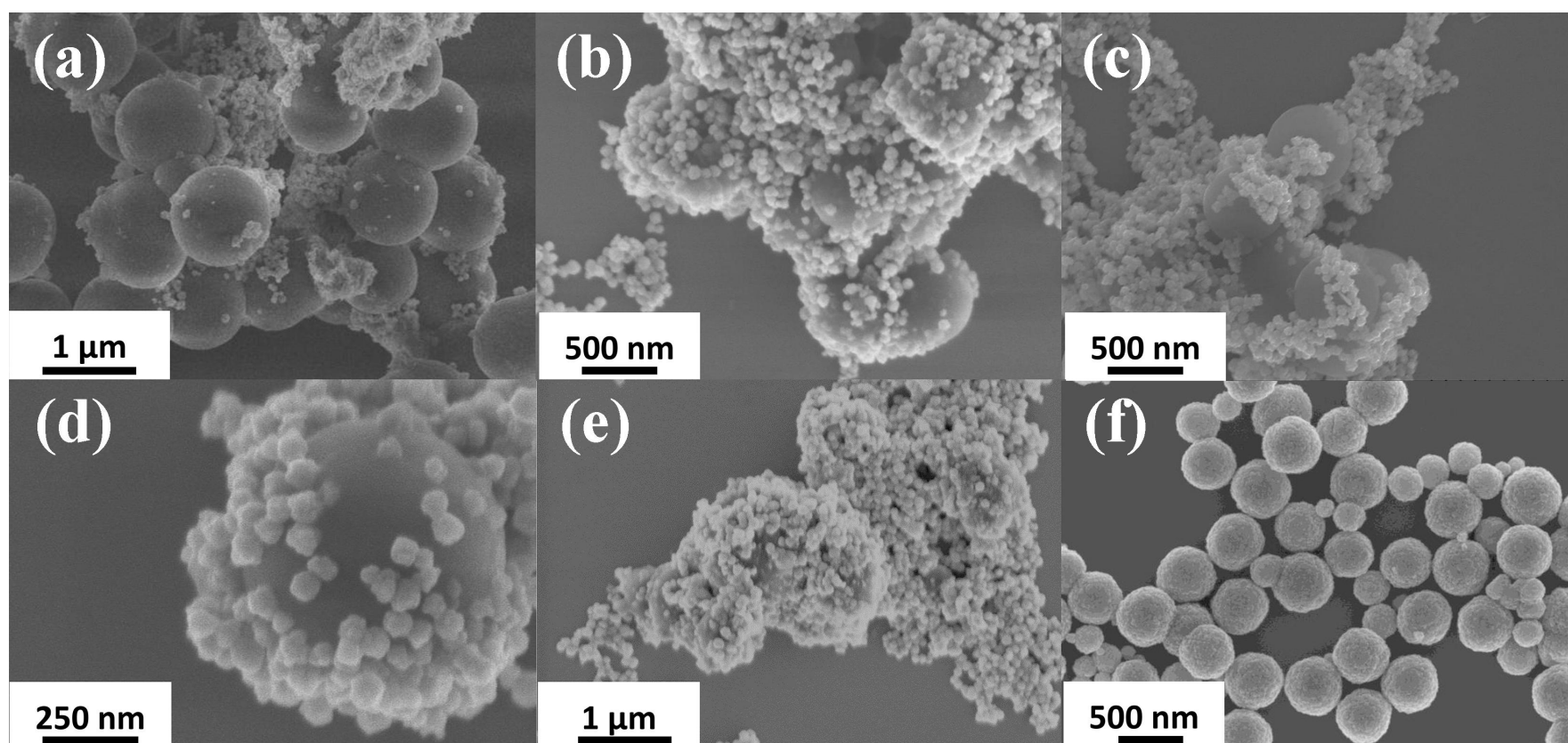


Fig. S2 SEM images of (a) RF/Fe₃O₄, (b) RF@ Fe₃O₄-6 h, (c) RF@ Fe₃O₄-12 h, (d) RF@ Fe₃O₄-1, (e) RF@ Fe₃O₄-3, and (f) Fe₃O₄ microspheres.

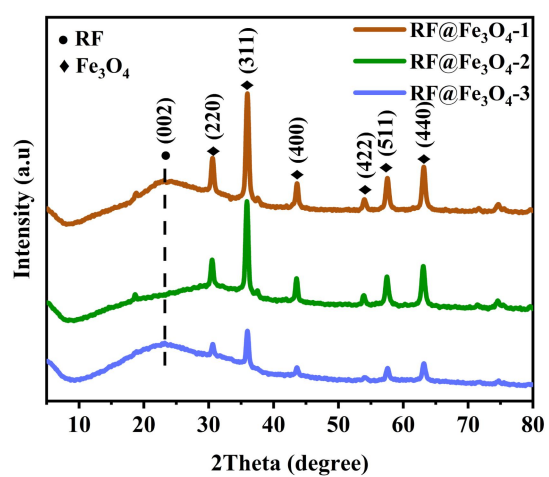


Fig. S3 XRD patterns of RF@Fe₃O₄-1, RF@Fe₃O₄-2 (RF@Fe₃O₄) and RF@Fe₃O₄-3.

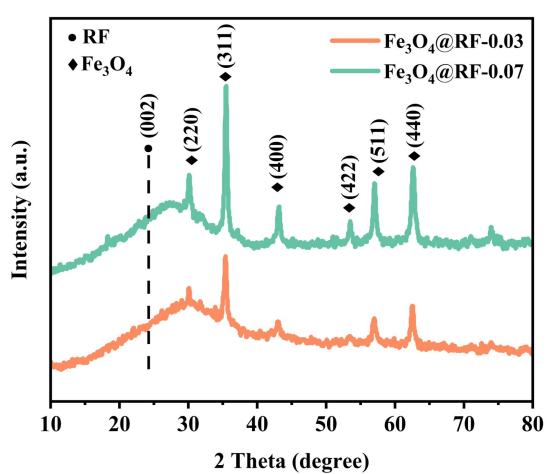


Fig. S4 XRD patterns of Fe₃O₄@RF-0.03 and Fe₃O₄@RF-0.07.

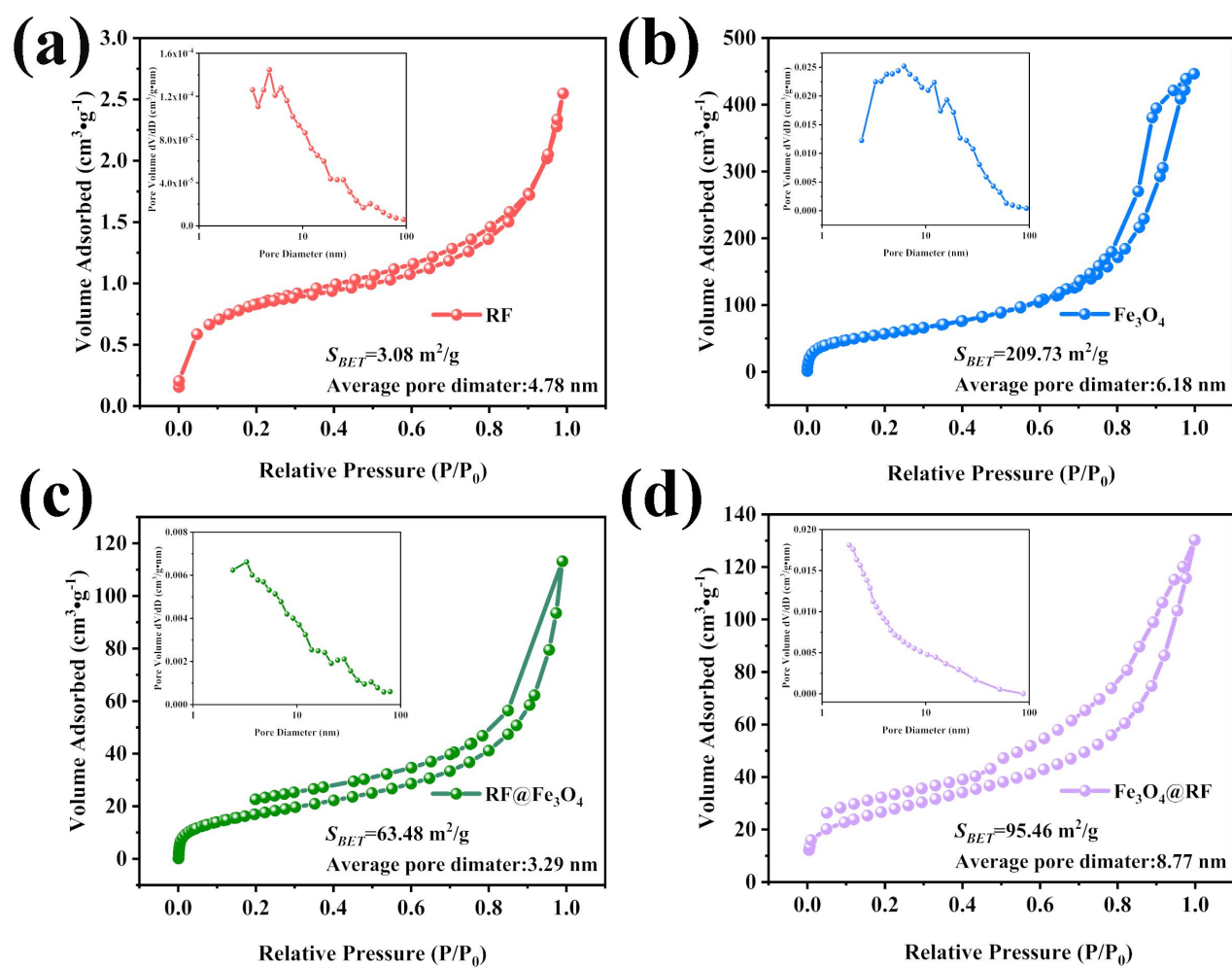


Fig. S5 N₂ adsorption-desorption isotherms and pore size distributions (inset) of (a) RF, (b) Fe₃O₄, (c) RF@Fe₃O₄, and (d) Fe₃O₄@RF.

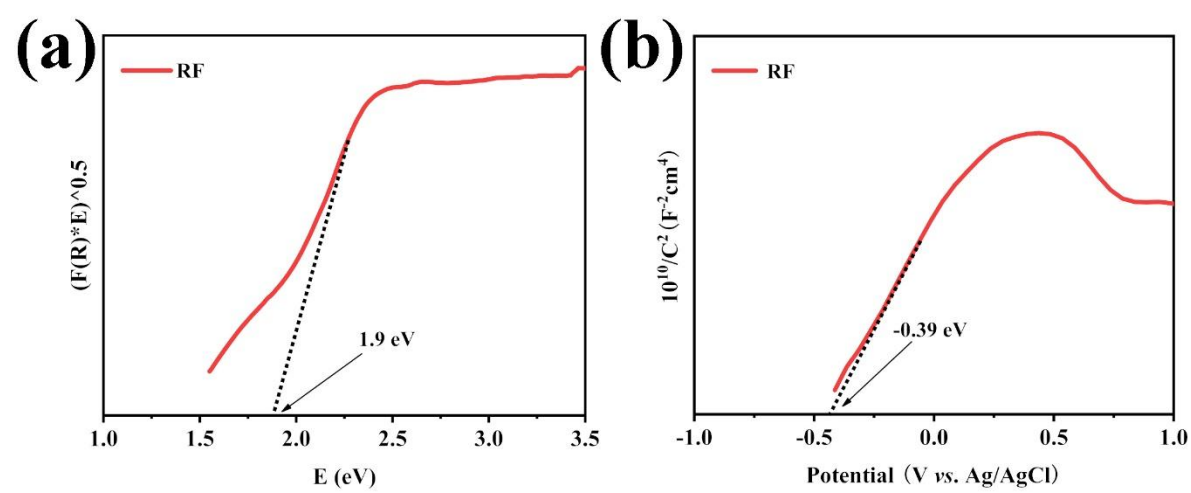


Fig. S6 (a) Corresponding band gap of the RF sample estimated by K-M function. (b) Mott-Schottky curve of the RF sample.

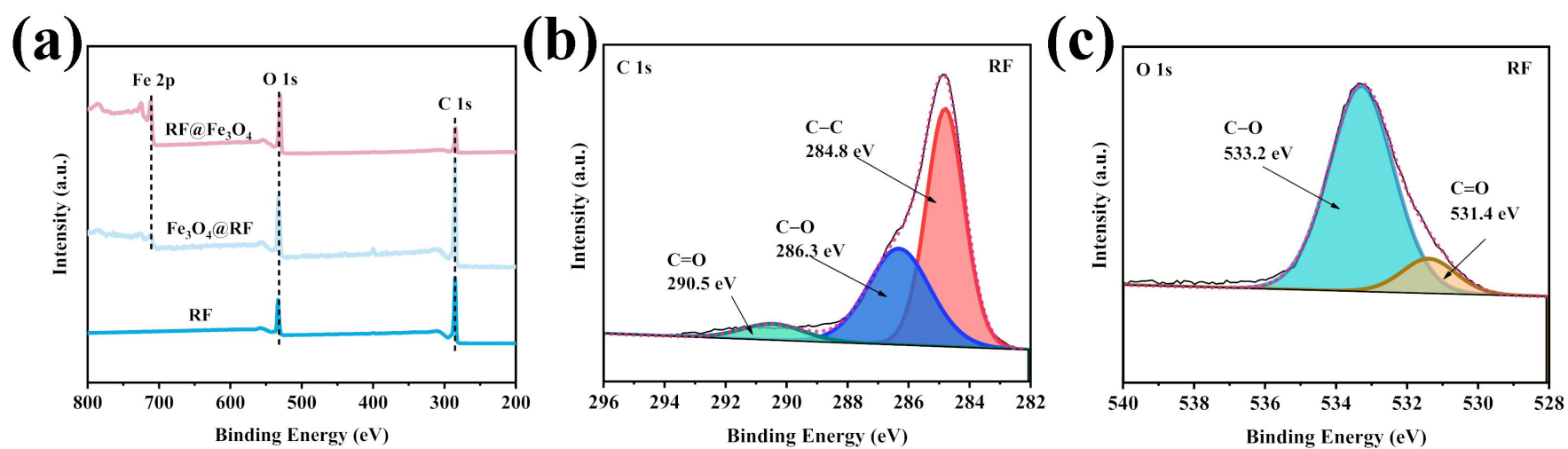


Fig. S7 XPS spectra: (a) survey spectra of the RF, RF@Fe₃O₄, and Fe₃O₄@RF samples; (b) C 1s and (c) O 1s spectra of the RF resin microspheres.

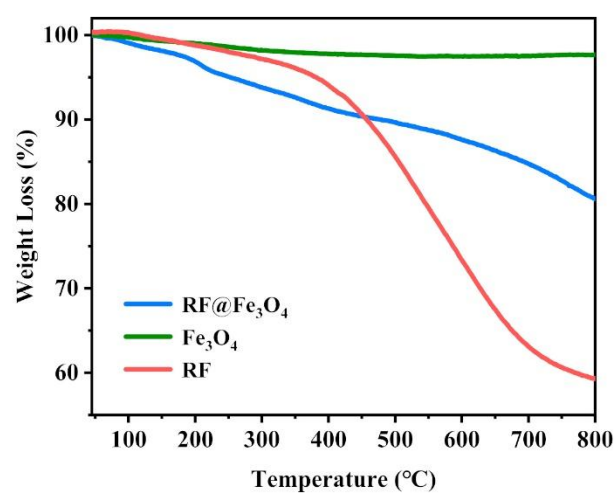


Fig. S8 TG curves of RF, Fe₃O₄ and RF@Fe₃O₄.

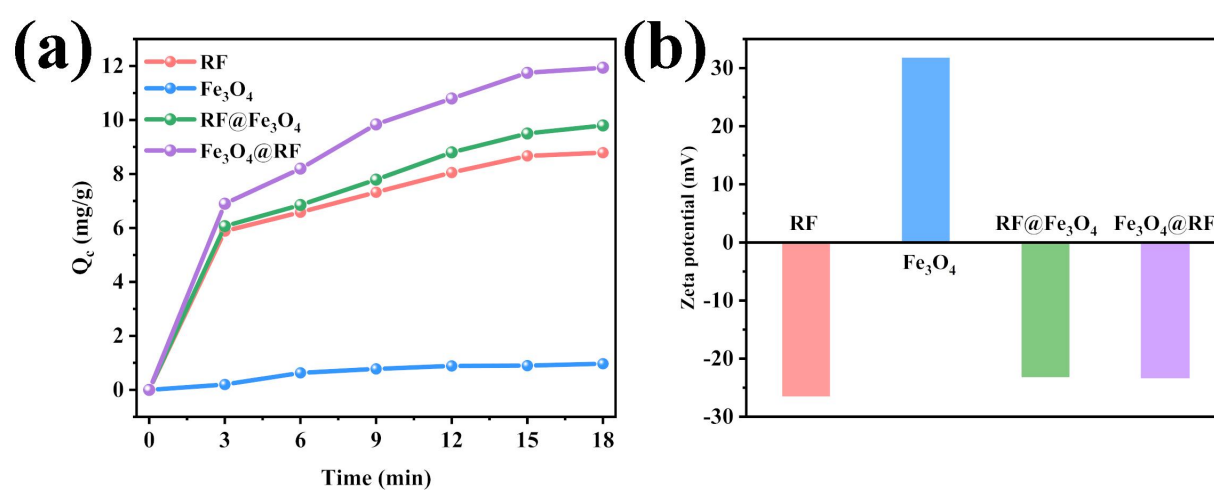


Fig. S9 (a) The adsorption capacities of the RF, Fe_3O_4 , $RF@Fe_3O_4$ and $Fe_3O_4@RF$ catalysts for MeB. (b) The zeta potentials of the RF, Fe_3O_4 , $RF@Fe_3O_4$ and $Fe_3O_4@RF$ catalysts in neutral solutions.

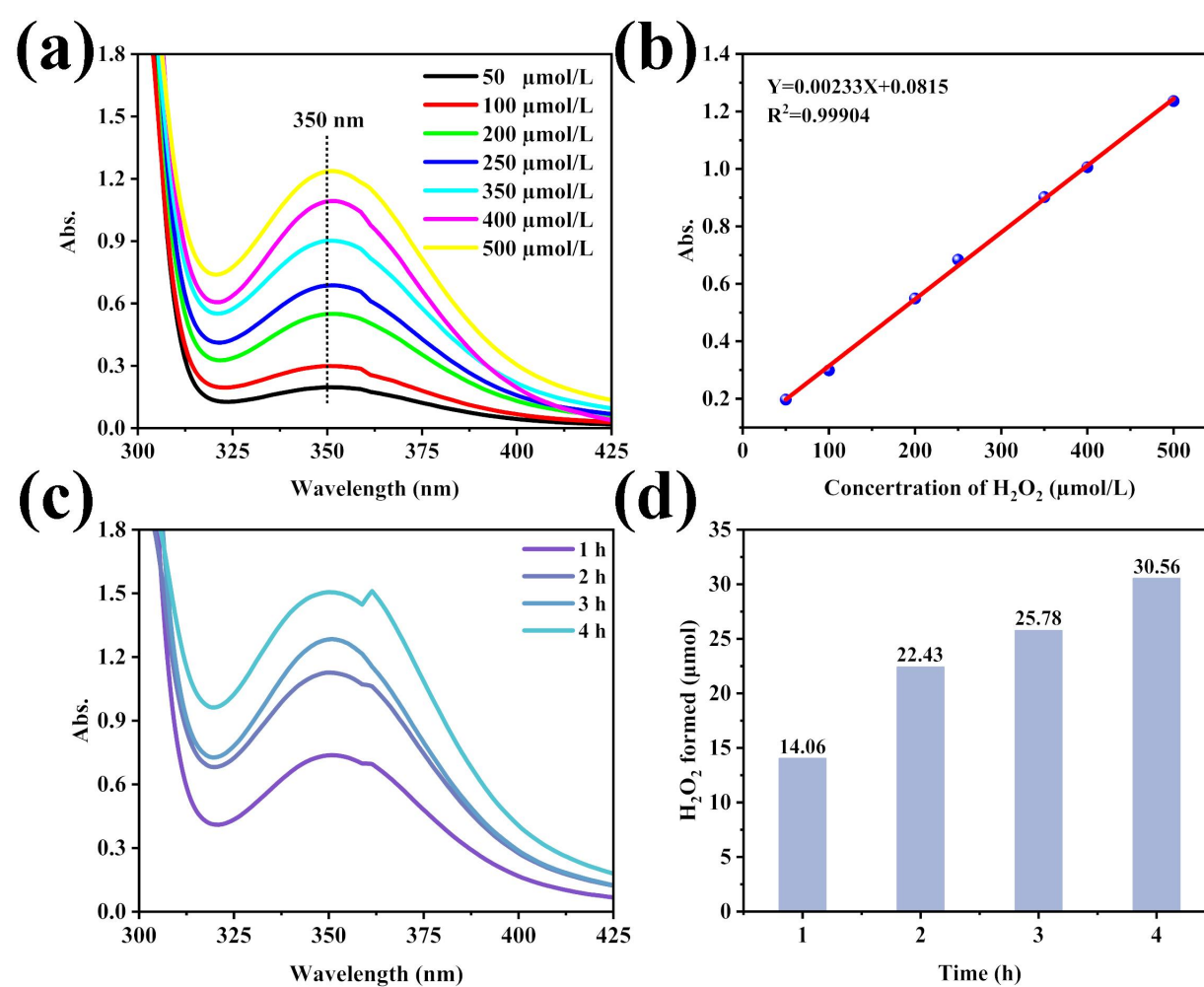


Fig. S10 (a) UV-vis absorption spectra of the standard H_2O_2 solutions measured by the iodometric method. (b) The corresponding standard curve of H_2O_2 concentration. (c) UV-vis absorption spectra of the produced H_2O_2 . (d) Amounts of H_2O_2 photogenerated by the RF resins.

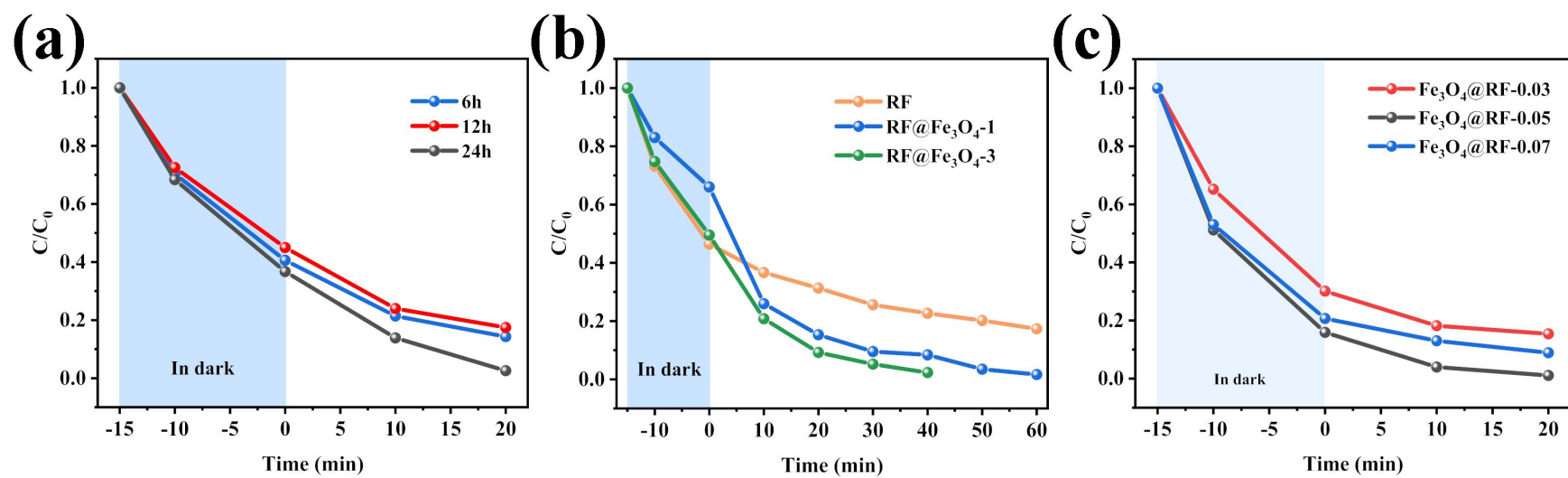


Fig. S11 (a) The time-course degradation of MeB by RF@Fe₃O₄ catalysts prepared with different sulfonation time. (b) The time-course degradation of MeB by RF, RF@Fe₃O₄-1 and RF@Fe₃O₄-3. (c) The time-course degradation of MeB by Fe₃O₄@RF-0.03, Fe₃O₄@RF-0.05(Fe₃O₄@RF) and Fe₃O₄@RF-0.07.

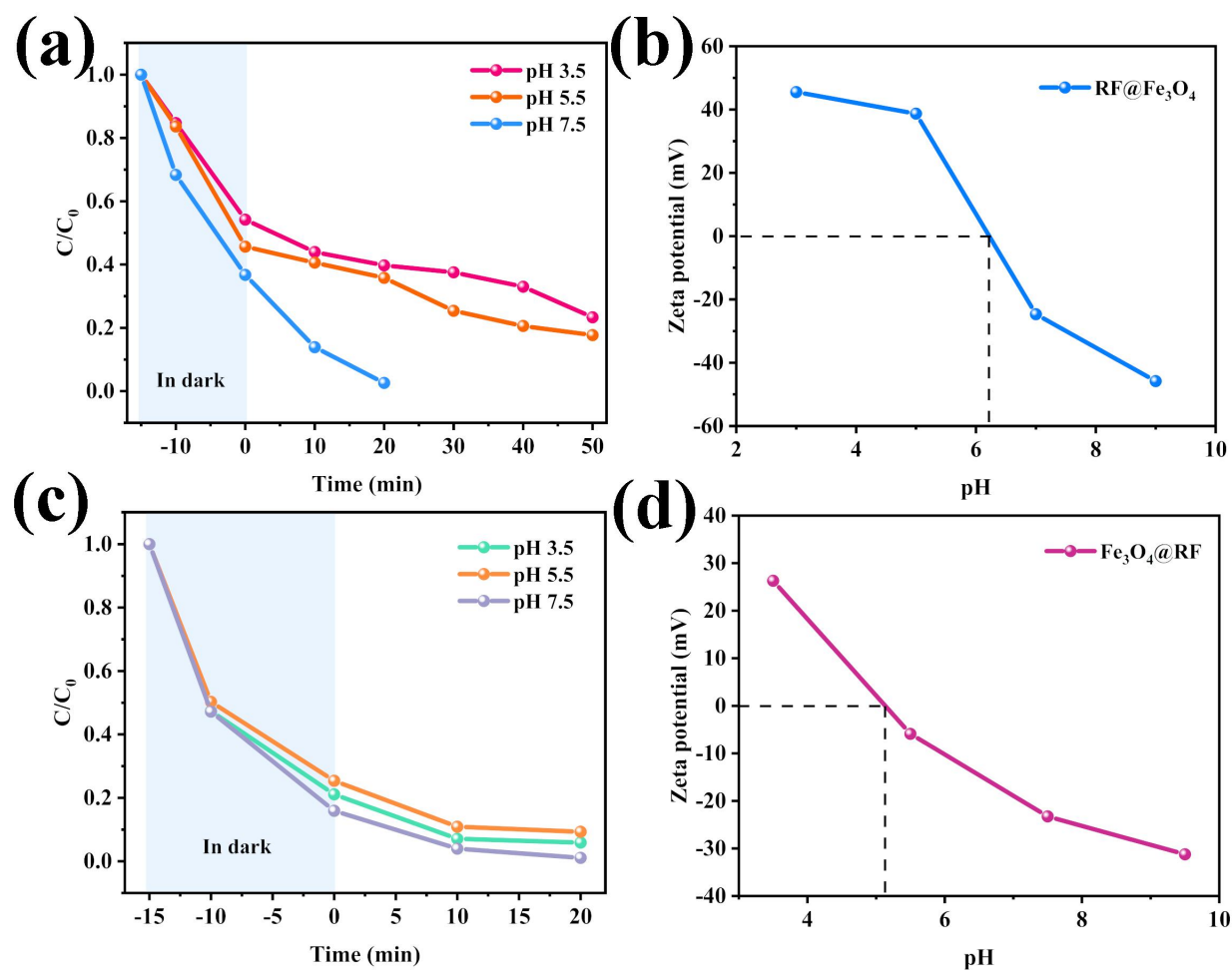


Fig. S12 The time-course degradation of MeB in the solution at different pH values by (a) RF@Fe₃O₄ and (c) Fe₃O₄@RF, and Zeta potential at different pH values of (b) RF@Fe₃O₄ and (d) Fe₃O₄@RF.

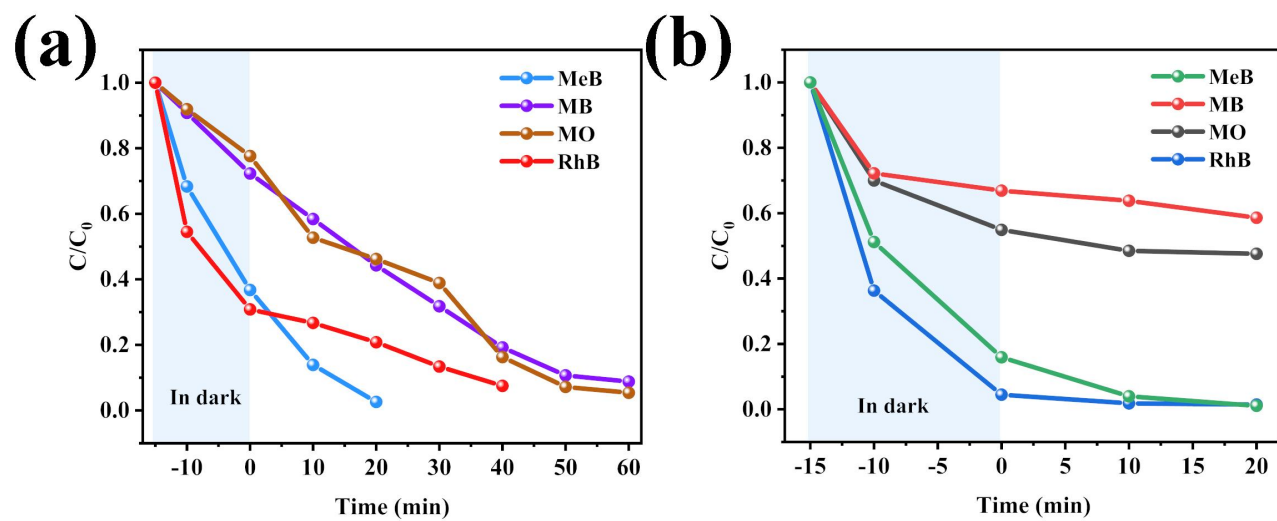


Fig. S13 The time-course degradation of different dyes by (a) RF@Fe₃O₄ and (b) Fe₃O₄@RF.

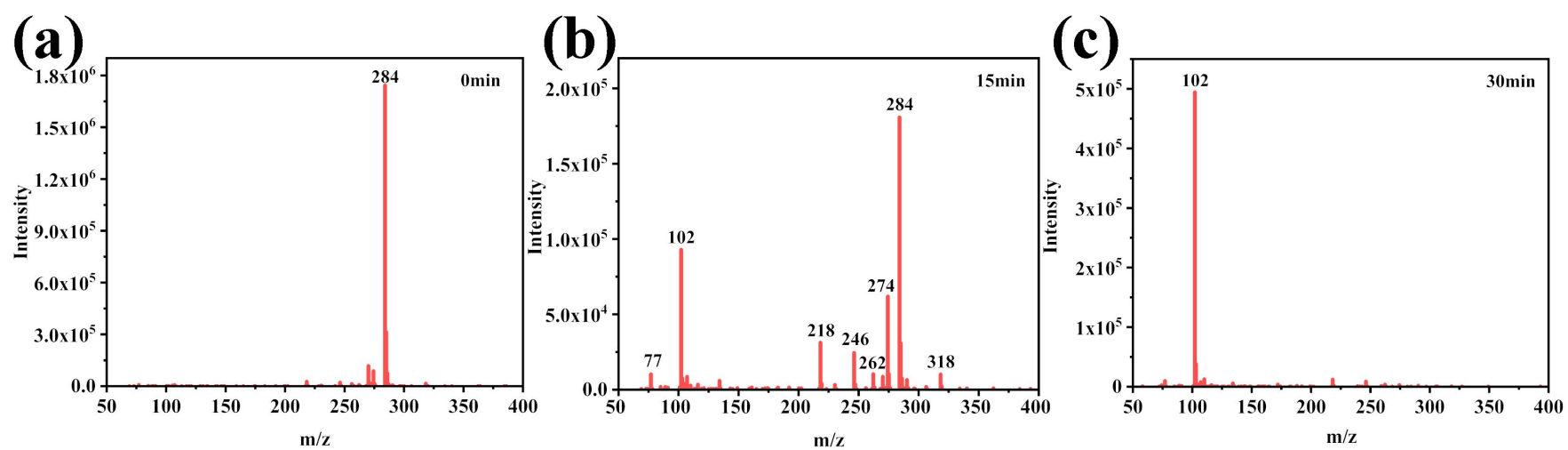


Fig. S14 The mass spectra signals of intermediates from decomposed MeB monitored at different time intervals: (a) 0 min, (b) 15 min, and (c) 30 min.

Table S1. Comparison on the reactivities by various catalysts.

Catalysts	k (min ⁻¹)	k (min ⁻¹ •w _{RF} % ⁻¹)	Efficiency	TOC removal efficiency
No catalysts, Dark	0.0013	/	5.7%	/
No catalysts, Light	0.0029	/	12.1%	/
RF	0.016	0.016	68.7%	14.9%
Fe ₃ O ₄	0.0017	/	10.5%	/
RF/Fe ₃ O ₄	0.0098	/	37.9%	/
RF@Fe ₃ O ₄	0.132	0.27	97.4%	42.6%
Fe ₃ O ₄ @RF	0.134	0.46	98.9%	54%

Experimental conditions: [MeB]=15 mg/L; [Catalyst]=1 g/L; pH=7.5; T=25 °C.